

# Open Research Online

---

The Open University's repository of research publications  
and other research outputs

## Prelaunch performance evaluation of the cometary experiment MUPUS-TP

### Journal Item

#### How to cite:

Marczewski, W.; Schroer, K.; Seiferlin, K.; Usovich, B.; Banaszkiewicz, M.; Hlond, M.; Grygorczuk, J.; Gadomski, S.; Krasowski, J.; Gregorczyk, W.; Kargl, G.; Hagermann, Axel; Ball, Andrew; Kuhrt, E.; Knollenberg, J. and Spohn, T. (2004). Prelaunch performance evaluation of the cometary experiment MUPUS-TP. *Journal of Geophysical Research: Planets*, 109(E7) E07S09.

For guidance on citations see [FAQs](#).

© [\[not recorded\]](#)

Version: [\[not recorded\]](#)

Link(s) to article on publisher's website:  
<http://dx.doi.org/doi:10.1029/2003JE002192>

---

Copyright and Moral Rights for the articles on this site are retained by the individual authors and/or other copyright owners. For more information on Open Research Online's data [policy](#) on reuse of materials please consult the policies page.

---

[oro.open.ac.uk](http://oro.open.ac.uk)

## Prelaunch performance evaluation of the cometary experiment MUPUS-TP

W. Marczewski,<sup>1</sup> K. Schröder,<sup>2</sup> K. Seiferlin,<sup>2,3</sup> B. Usowicz,<sup>4</sup> M. Banaszkiewicz,<sup>1</sup>  
M. Hlond,<sup>1</sup> J. Grygorczuk,<sup>1</sup> S. Gadomski,<sup>1</sup> J. Krasowski,<sup>1</sup> W. Gregorczyk,<sup>5</sup> G. Kargl,<sup>6</sup>  
A. Hagermann,<sup>7</sup> A. J. Ball,<sup>7</sup> E. Kürt,<sup>8</sup> J. Knollenberg,<sup>8</sup> and T. Spohn<sup>2</sup>

Received 3 October 2003; revised 4 March 2004; accepted 30 March 2004; published 8 July 2004.

[1] This paper discusses test results obtained in both laboratory and terrestrial environment conditions for the “Multipurpose Sensors for Surface and Sub-Surface Science” Thermal Probe (MUPUS-TP), which has been developed for the European Space Agency Rosetta cometary rendezvous mission. The probe is intended to provide in situ long-term observations of the thermal evolution of the comet nucleus and will measure a thermal conductivity profile with time in the top 30 cm of the comet nucleus. The basic operating principles of the probe are briefly described, including typical test results gathered in terrestrial snow and soil. The tests in snow provide verification of the probe as a useful tool for monitoring the metamorphism of snow on the Earth. The tests in soil are intended to demonstrate the probe’s suitability as an alternative to other methods of energy measurement currently practiced in soil physics research. The tests of the probe in the natural environment of the Earth provide a demonstration of the behavior of the instrument in the presence of complex energy exchange processes before it is used on the comet.

**INDEX TERMS:** 6210 Planetology: Solar System Objects: Comets; 6297 Planetology: Solar System Objects: Instruments and techniques; 5470 Planetology: Solid Surface Planets: Surface materials and properties; 5494 Planetology: Solid Surface Planets: Instruments and techniques;  
**KEYWORDS:** energy exchange, heat diffusion, thermal conductivity

**Citation:** Marczewski, W., et al. (2004), Prelaunch performance evaluation of the cometary experiment MUPUS-TP, *J. Geophys. Res.*, 109, E07S09, doi:10.1029/2003JE002192.

### 1. Introduction

[2] An important goal of current research in planetology and earth sciences is the identification and understanding of the physical processes powered by energy exchange and their dynamics. The focus is first on the identification of the material’s components, their structure and texture, and finally on their origin. There is also a strong interest in the evolution of the forms and the processes determining morphology.

[3] A common factor in all of these research areas is the need to understand the thermal properties and the mass and energy transport of the media under study. MUPUS officially means the program of “Multipurpose Sensors for Surface and Sub-Surface Science” operating the Thermal Probe (TP) to measure the temperature field and thermal conductivity in a one-dimensional (1-D) spatial distribu-

tion. Essentially the bulk conductivity of the media is derived from the measurement results. The probe is an element of the complex penetrator built for the MUPUS program. The probe MUPUS-TP and the measurement method were proposed by the MUPUS team (T. Spohn, MUPUS Proposal, 1995, Institut für Planetologie, WWU, Münster. Available online at <http://ifp.uni-muenster.de/pp/MUPUS/mupus-proposal.pdf>) [Spohn et al., 1995] as a program for thermal research and were accepted for the European Space Agency (ESA) Rosetta cometary mission.

[4] The space experiment MUPUS was developed at, and is supported by, the Institut für Planetologie (IfP) Westfälische Wilhelms-Universität (WWU), Münster, Germany. The project is conducted by T. Spohn (IfP) and K. Seiferlin (IfP). Technical design and engineering development of the probe were performed at the Space Research Centre (SRC), Warsaw, Poland.

[5] The EXTASE program was defined by and is carried out at the IfP, WWU, as a spin-off of the MUPUS project. The goal of this program is to be developed further and apply the MUPUS-TP probe technology and measurement methodology to Earth sciences. Design of the equipment and engineering support is provided by SRC, Warsaw, Poland.

[6] The space experiment will be performed on the comet 67P/Churyumov-Gerasimenko in the year 2014 and until that time experience with the probe and related measurement interpretation will be obtained in the terrestrial environment. The probe has recently undergone

<sup>1</sup>Space Research Centre, Polish Academy of Sciences, Warsaw, Poland.

<sup>2</sup>Institut für Planetologie, Westfälische Wilhelms-Universität Münster, Münster, Germany.

<sup>3</sup>Now at Physikalisches Institut, Bern, Switzerland.

<sup>4</sup>Institute of Agrophysics, Lublin, Poland.

<sup>5</sup>Telecommunication Research Institute, PIT, Warsaw, Poland.

<sup>6</sup>Institut für Weltraumforschung, Graz, Austria.

<sup>7</sup>Planetary and Space Sciences Research Institute (PSSRI), Open University, Milton Keynes, UK.

<sup>8</sup>DLR, Berlin, Germany.

extensive testing in different terrestrial conditions, both in the laboratory and in the terrestrial environment, in order to verify that it complies with the mission requirements. A detailed description of the probe and the sensor package is beyond the scope of the present paper and will be given elsewhere. Here we report on test campaigns with the probe in snow and soil and discuss the layout of the probe only briefly.

[7] The paper comprises nine sections. Section 1 discusses arguments concerning in situ investigations in order to study the thermal and energy exchange processes below the surface of the medium. The basic technology of the MUPUS-TP probe and the measurement method are described in section 3. Section 4 explains the concept of operating the TP probe. The timing conditioning of the probe is explained in section 5 using the examples of the heat and mass flow. These aspects of the methodology are illustrated by simple tests to clarify how the probe will be applied to study the comet. Section 6 discusses the question of the relevance of the thermal study using the probe to the actual physical state of the media, specifically considering the example of the latent heat effects related to water ice. Section 7 focuses the discussion on another aspect of the geometrical configuration of the probe aligned with the direction of the heat flux under sensing. Section 8 turns to the terrestrial applications of the probe in a snow environment, and section 9 considers using the probe for the heat flux determination in the soil environment. The paper closes with a review of the potential and capabilities of the method, giving relevant conclusions in section 10.

## 2. Why Investigate In Situ Instead of Remote Sensing?

[8] In general, the energy balance is given by following constituents: the incoming solar radiation and the radiation outgoing from the body, the heat diffusion inside bulk material, and the heat flow accompanying mass transport and phase transitions all that determined at the surface of the body. The temperature distribution of the medium is an observable quantity providing direct information about the thermal state and the heat flow processes. One standard method for getting the temperature distribution near the surface of a body is to employ remote radiometric observations (e.g., IR or microwaves).

[9] Radiometers measure the emitted radiation of an object and by applying Planck's law its brightness temperature. The brightness temperature is a property related to the physical temperature of the body by the surface emissivity. The observations are used to characterize the superficial layers of the target body down to a certain depth depending on the wavelength of the radiation and the absorption properties of the medium. The surface temperature, which can be derived from remote sensing, is affected by deeper layers of the object within a thickness of the order of few thermal skin depths. Therefore the information on the thermal properties of the target that can be gained by remote sensing is restricted to this depth range, typically being in the mm to cm-range for the diurnal cometary heat wave. Furthermore, remote observations can directly only deliver the

thermal inertia  $((\lambda \cdot \rho \cdot c)^{1/2})$ ,  $\lambda$  = thermal conductivity,  $\rho$  = bulk density,  $c$  = heat capacity) of the uppermost target layers. To derive the basic property thermal conductivity, additional information about the bulk density and heat capacity of the material is needed. In the case of microwave observations knowledge of the electrical properties of the material is also required. Another problem of remote sensing is the not well known atmosphere of the target. All these unknowns contaminate the radiation measurements. Then, one must employ complex correction procedures to characterize the subsurface phenomena using the radiation transfer equation well known from radio astronomy [Rohlfs, 1986]. Furthermore, remote sensing cannot provide data from the same area at short time intervals. First, this is important to get a good approximation of the body's wavelength-dependent emissivity and therefore to derive an accurate estimate of the physical temperature from the data. In addition, possible temporal changes (e.g., due to changes in cometary activity) of the thermal and physical properties at the landing site can also be characterized at best crudely by remote observations. Consequently, remote sensing observations cannot replace in situ investigations, which are the only means to provide the important thermal and physical parameters of the comet with the desired accuracy and over the relevant depth range.

[10] On the other hand, it is known from Keihm [1984] that even the seemingly simple task of estimating the heat flow from remote observations of bodies with well-known bulk surface properties and thereby the well-defined heat transfer processes, requires a large amount of prior information on optical and other properties of the surface. Therefore the results inferred from remote observations are highly model dependent.

[11] On the Rosetta mission there are two remote sensing instruments that detect the target's emissions: VIRTIS (a Visible Infra Red Thermal Imaging Spectrometer is provided by CNR IASF), for IR imaging of the comet, and MIRO (Microwave Instrument for the Rosetta Orbiter provided by JPL) for the millimeter and sub millimeter radiation.

[12] The probe MUPUS-TP is intended to support the studies of the energy exchange locally inside the medium, by measurements of the temperature field and thermal conductivity as a function of time and depth. Other properties such as structure, texture, mass transport, etc., may be interpreted independently of the apparent thermal effects with the aid of other physical knowledge and observations. These are general aims of the experiment MUPUS-TP, developed for investigating a cometary nucleus. Similar aims may be defined also for earth sciences.

## 3. Thermal Probe and the Method

[13] This section describes the operation of the probe and the basic measurement methodology. There are two independent aspects of the probe and the method. The first is the time dynamics of the reaction between the sensor and the medium. The second is the coupling of the probe and the medium, which is determined by the initial conditions, geometrical boundaries and the related temperature field.

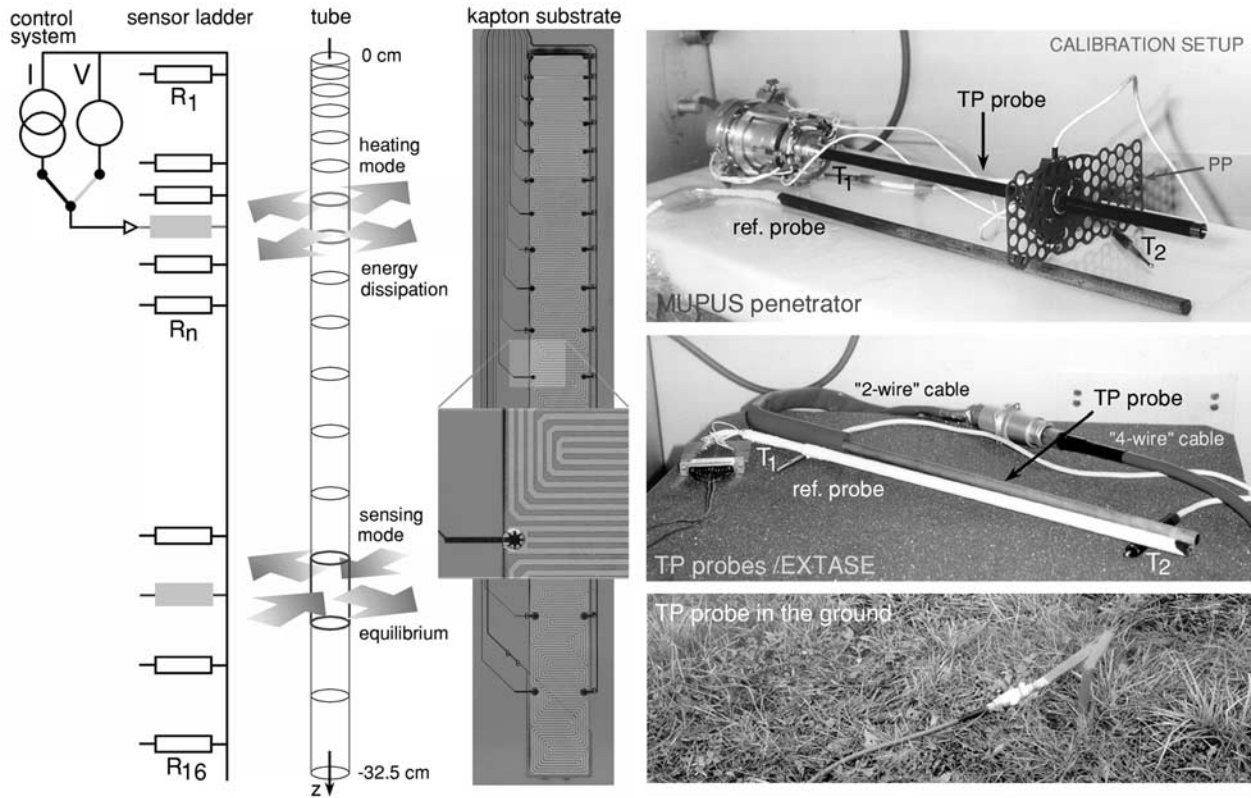


**Figure 1.** General scheme and configuration of the MUPUS-TP sensors (left), a photo of the Kapton substrate with sensors (middle) with a detail (inset), and other photos showing penetrator and probes in a calibration setup (top right) and the probe in soil (bottom right). The space instrument is equipped with the PP (Permittivity Probe) antenna (the wide rectangular wing) provided by the experiment SESAME/PP designed for the dielectric permittivity measurements (the photo at top right). See color version of this figure in the HTML.

[14] The measurement methodology of the MUPUS-TP probe was inspired by the technique of a linear heat source, also known as “the hot wire method,” from the ASTM (D5334-92 1992) and IEEE (Std. 442-1981) standards. This method assumes a negligibly thin linear heat source implemented in the medium, and predicts the time dynamics in the behavior of the system.

[15] The method of the MUPUS-TP experiment essentially assumes the same kind of time dynamic behavior but relaxes the requirement on the negligibly thin geometry of the probe. The usefulness of the linear heat source method for the TP concept was studied first by *Seiferlin et al.* [1996] and subsequently by *Banaszkiewicz et al.* [1997]. *Hagermann* [1999] performed the first study on the temperature field distribution and the temperature gradient conditioning for a probe and its cylindrical geometry.

[16] The standard method assumes that a linear source dissipates the heat into a homogeneous medium, with a resulting temperature rise in the surrounding media. It is assumed that the medium is infinite in extent in comparison to the geometry of the wire. The temperature increase,  $\Delta T$ , is the main observable quantity. The heat input is maintained until the slope of  $\Delta T$  in the logarithmic measure of time, becomes constant. If the dissipated power,  $P$ , is constant and a uniform heat distribution around and along the wire of the length,  $l$ , is achieved, then the thermal

conductivity  $\lambda$  of the medium is possible to determine (as described by *Healy et al.* [1976]) and is given by the following equation:

$$\lambda = \frac{P}{4\pi l} \frac{d \ln(t)}{dT}. \quad (1)$$

[17] The standard method employs a single element for sensing and heating in one operation. The heating of the wire is characterized by the current,  $I$ , and the voltage,  $V$ , on the wire while the thermal effect of heating the medium is covered in the time dependence of the temperature increase  $\Delta T$ . This standard approach cannot supply information regarding the spatial distribution of the thermal state and properties of the medium along the wire.

[18] The approach employed for the MUPUS-TP probe, while based on this standard approach, aims to extend the methodology to allow for the measurement of the spatial distribution of the thermal properties. The TP probe does not utilize a single wire. Instead, it is a linear series of many toroidal units, and the theory of a probe in this configuration did not exist before. The probe consists of a series of independent RTD (Resistance Temperature Dependent) sensors as shown in Figure 1. The same sensor elements are employed for the functions of sensing and heating.



[19] Each sensor element is sampled using a constant current source,  $I$ , in order to obtain a measurement of the temperature  $T$ . The same element is heated by a constant voltage source,  $V$ , when employed for a measurement of the thermal conductivity  $\lambda$ . The functions are separated by time multiplexing their operation. Since the RTD sensor varies its resistance when heated, the power dissipated varies with time, but the rate of change is known and controlled quantitatively. The value of  $\lambda$  is derived by observing the time when the logarithmic time slope of the temperature increase,  $dT/d(\ln(t))$ , achieves a steady value.

[20] In order to make temperature measurements, the heating cycle is interrupted for a few milliseconds, which has no effect on the heating. The total heating cycle is usually many minutes and the temperature measurements take only a few seconds or less. For the temperature measurements the sensors are sampled with short current pulses of 20 mA and 16 pulses are averaged together for a single reported measurement. The heat is pumped in a series of current pulses repeated with the period of 84  $\mu$ sec. The power rate is controlled by the repetition rate of the pulses. The control system utilizes 14-bit resolution for the sensing mode, and 12-bit resolution for the power rate in the heat pumping mode. The available power for pumping is about 1 W. This results in a temperature resolution of better than 0.05°C. The temperature precision is about 0.1°C. The method relies on the measurement of the temperature increase. Even the less precision is not critical for the method. The range of measured temperature values is presumed for the comet to be about  $-160^{\circ}\text{C}$  to  $+100^{\circ}\text{C}$ . The sensors are not required to be equal in resistance. It is sufficient to know their temperature-dependent characteristics from calibration data. The resistance of the sensors is around 100 Ohm.

[21] The MUPUS-TP probe contains a linear series of sixteen toroidal units arranged in a common cylinder 32.5 cm long. Each of these units is “short and thick” with respect to the diameter (10 mm) of the probe (Figure 1). A series of such toroidal units, is a complex analog of the single wire. It is intended to transect the medium by a linear series of sensors and heaters. The probe is able to sense the 1-D temperature field axially but it is azimuthally insensitive. If one sensor does not disturb another, the probe reacts to the heat flowing parallel to the probe. The value of thermal self-conductivity of the probe is minimized as much as possible.

[22] The thermal conductivity of the probe is determined first by the conductors. The electrical layout the probe is a ladder of 16 sensors connected to the control system by a single common conductor and 16 others addressed to sensors. This layout enables the use of the two-wire method for resistance measurements. The two-wire method minimizes the number of conductors in the ladder. The design employs a thin film technology, in order to reduce heat capacity of the sensors. The total amount of metal material for the probe is about 3 g. The sensors are created on one integral common sheet of the Kapton substrate and encapsulated between two other Kapton layers 50  $\mu$ m thick. The substrate is processed flat and then it is wound in a multilayer spiral inset and bonded to the tube walls from the inner side of the cylindrical tube. The resistive material of the sensors is titanium, laid in a thin metal clad about 0.5  $\mu$ m thick. The probe reacts

thermally to the exterior through the sidewall of the tube. The overall thermally active area of the probe is large, about 1 dm<sup>2</sup> in total. The wall is made of a cyanato-ester composite filled with fiberglass 1 mm thick. The composite is a poor heat conductor.

[23] The placement of the sensors inside the tube seems inconsistent with the requirement for minimal thermal resistance to the outside. This overall design solution is a compromise between thermal considerations and fabrication methods. In addition to the thermal performance requirements the penetrator, for the Rosetta mission, is required to withstand the strong mechanical action of hammering the tube into the medium from the top side (the probe is inserted into the surface like a nail). If the design had placed the sensor layer outside the wall then there would be the risk of axially cutting the layer as a result of the elastic strain waves traveling along the tube due to the shock of hammering. The shock wave can cause higher strain on the outside skin at the diameter 10 mm, than on the inner side at the diameter 8 mm. Another risk for the sensor would be the friction between the outer wall of the tube and the surrounding medium. In general the thin film sensors are sensitive to strains and for this reason the probe has the form of a stiff tube. The insertion of the probe in terrestrial use may be safely aided by first drilling a hole in the medium, thus eliminating the need for hammering. However, we did not pursue a design with the sensors outside the tube. On the basis of a quantitative analysis of the thermal design, depending on the ratio of the tube wall thickness to the length of a single sensor, the impact of placing the sensors along the inner tube wall was not deemed to be significant in the thermal conditions encountered on Earth. Placing the sensors outside the probe only has an impact in the case of a very well-conducting probe in a medium of extremely small conductivity.

[24] The probe was calibrated on the temperature-dependent resistance in several specimens and then examined for operations of sensing and heating. Temperature-dependent resistance  $R(T)$  was assumed to be a linear function

$$R(T) = R_0(1 + s \cdot \Delta T + s_1 \cdot \Delta T^2 + s_2 \cdot \Delta T^3), \quad (2)$$

where  $R_0 = R(T_0 = 0^{\circ}\text{C})$ ,  $\Delta T = T - T_0$  (difference to  $0^{\circ}\text{C}$ ), and  $s = (R(T)/R_0 - 1)/\Delta T$  – is the normalized temperature sensitivity.

[25] The sensitivity of a typical RDT is  $s = 3.85 \times 10^{-3} \text{ K}^{-1}$  (for a commercial PT100) in absolute measure. Sensors of the MUPUS-TP probe have a typical sensitivity of about  $2 \times 10^{-3} \text{ K}^{-1}$ . Titanium belongs to the group of metals that are well behaved in the range of temperature  $-160^{\circ}\text{C}$  to  $+100^{\circ}\text{C}$  and adequately fit a linear model. The sensitivity value,  $s$ , for the sensor is reduced to about a half of the value corresponding to the bulk metal of titanium. The reduction is due to a structural difference of the thin layer 0.5  $\mu$ m thick. The reduced value of sensitivity does not limit the measurement as much as the disturbance by the heat conduction along the wires, the sensors and the heat capacity of the metal layer.

[26] The normal position of the probe in operation is perpendicular to the surface of the ground. The steepest gradient of temperature in the ground is expected close to

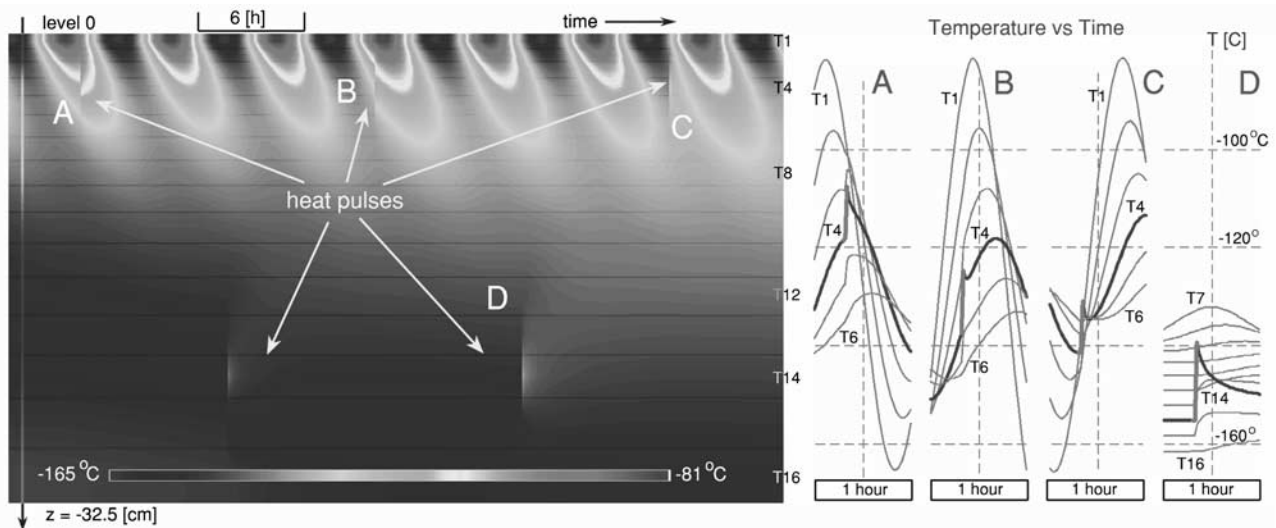


**Figure 2.** This is example data from 16 sensors of the probe MUPUS-TP in a simulated observation of diurnal cycling on the comet, including short instrumental heat pulsing. The map employs linear interpolation along the depth coordinate. The bulk conductivity of the ground is  $\lambda = 0.25$  W/m/K, the period of rotation is 6 hours, and a time step of the model calculation is 5 min. The color map (left) represents temperature versus time and depth. The rectangular plot (right) shows the effects of heat pumping in 1 hour intervals in different phases of a diurnal cycle. See color version of this figure in the HTML.

the surface. Thus it is preferred that the top layers are thermally sampled with a smaller increment and higher spatial resolution than the bottom layers. In order to achieve this goal the length of each of the sensors varies logarithmically along the length of the probe and they are adjacent one to another. There are no gaps between the sensors. Thus the full area of the probe is utilized. Each sensor is about 11% longer than the previous one, going down the probe (see Figure 1, left and middle). In effect the entire probe length of 32.5 cm long is fully covered with a series of sensors, of the length varying from 9 mm to 40 mm going from top to bottom. Thus one can consider that the undesired heat conducting path along a sensor is at least one order longer (for the top end sensor), than the path across the wall of the thickness of 1 mm. This is the simplest explanation. More thermal consequences of the wall are discussed on the basis of analysis results in the Section 7.

[27] The design and technology of the sensors are described by *Gregorczyk et al.* [1999]. The thin film technology on the Kapton substrate was developed in the Telecommunication Research Institute, PIT, Warsaw, Poland. The key problem was with finding a proper order of metal layers in the area where the thin film ( $<0.5$   $\mu\text{m}$ ) titanium clad interfaces the thick film copper clad ( $\sim 17.5$   $\mu\text{m}$ ) of conductors on the substrate. It was solved by a using intermediate thin film ( $<0.5$   $\mu\text{m}$ ) copper clads, laid from the bottom and the top sides of the titanium. The area of sensor contacts was very critical and it was developed to be as large as possible, using a star shape of the contact (shown in Figure 1, inset) inside a circle of the diameter 2–4 mm, depending on the sensor.

[28] First prototypes of the thin film sensors were made in 1998 and since that time the technology was further

optimized, in particular to control the effects of annealing and aging. The needs of the space mission require keeping the reference model to monitor the aging.

#### 4. Concept of Operation of the MUPUS-TP Probe

[29] A general overview of the goals of the MUPUS-TP experiment is given in the paper by *Kömle et al.* [2002]. They demonstrate the ability to detect the diurnal thermal cycling of a comet using the probe and the general measurement methodology. The thermal cycling was simulated for the comet Wirtanen by W. Seiferlin in 1999 (see Figure 2). The simulation assumes a six-hours period of rotation of the nucleus, an initial surface temperature about  $-165^\circ\text{C}$  and a bulk homogeneous medium. The bulk conductivity of the medium was assumed to be  $\lambda = 0.25$  W/m/K, representing mainly means of the heat transfer.

[30] The color map in Figure 2 shows an example of the expected temperature distribution down to 32.5 cm below the surface in 16 levels corresponding to the sensors, and the time history of cycles with a period of 6 h. The evolution of the temperature in time is similar to results regularly obtained in the terrestrial environment, differing only in periodicity and range of temperatures. The data is a simple 1-D finite difference model, started with an isothermal comet nucleus, and cannot be understood as a model describing the thermal evolution of the nucleus. Here it illustrates only the operation of the probe under conditions varying in time.

[31] The simulations illustrate also the phases of probing the thermal diffusivity (or conductivity) of the medium using heat pulses along the probe. Several pulses are shown in Figure 2, applied at two levels:  $-3.6$  cm and  $-23.6$  cm below the surface, and corresponding to the sensors T4 and

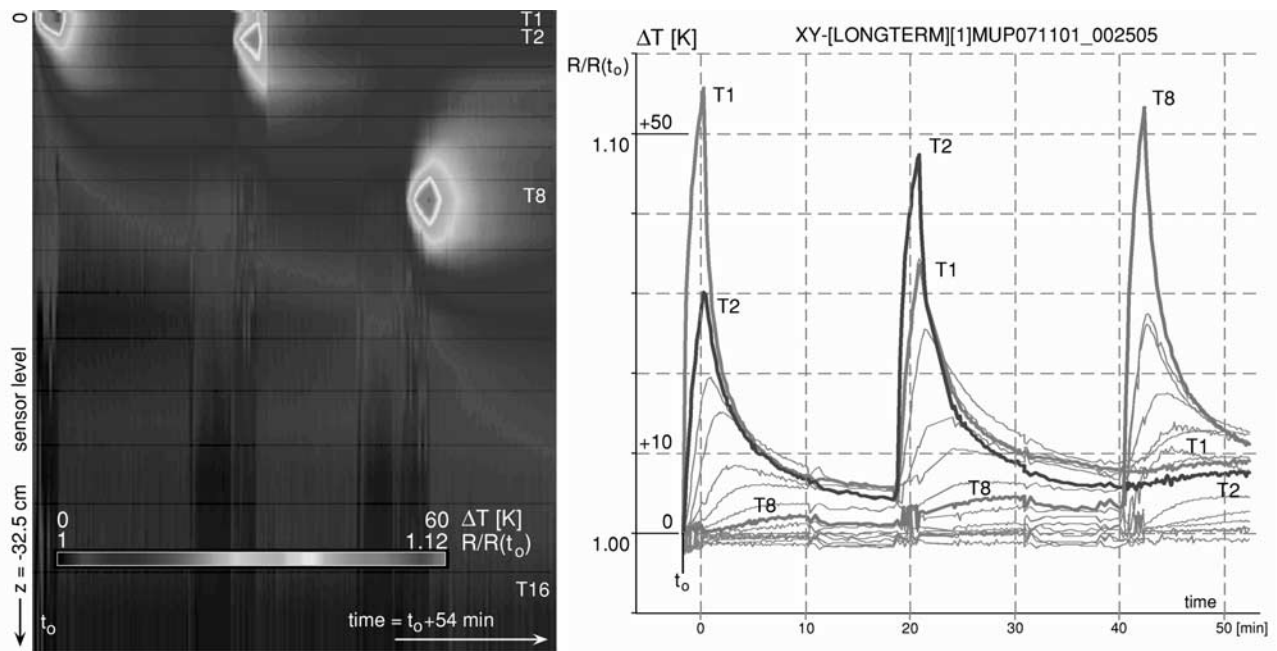


**Figure 3.** Test results of heat pulsing applied to the probe in vacuum with a cold background. The color map (left) shows the overall effect of “pumping the heat.” The effects are expressed in terms of a resistance change, in the values normalized to the resistance at the time when the pumping started. The rectangular plot on the right side shows the same intervals when a single sensor is heated (T1, T2, T8) while all the sensors are sensed. See color version of this figure in the HTML.

T14, respectively. The effects of the pulsing are visible as abrupt discontinuities on the map affecting diurnal natural cycles. The discontinuities indicate where in time the pulse occurred and moving from left to right, shows the artificial heat flow. The effects are also shown in another form on the rectangular temperature plot versus time, for the corresponding sensors and in three selected 1 h intervals. The temperature rises in a few minutes of the pulse and then decays in about half an hour.

[32] The diurnal solar cycle potentially provides another indirect opportunity to measure the rate of heat diffusion and thermal conductivity. This approach requires knowledge of the external energy input from other observations. However, the remote sensing experiments are not suited to determine the time-variable conditions at the test site.

[33] There is another instrument named MUPUS-TM (Thermal Mapper) on the Rosetta Lander which is better matched to that purpose. It is an infrared radiometer developed by E. Kührt and J. Knollenberg from DLR, Berlin. By measuring the infrared radiation emitted from a surface element of about 1 m<sup>2</sup> size at the landing site in four wavelength bands with high-temperature resolution down to 100°K, a good estimate of the absolute surface temperature as a function of time can be obtained. A direct estimate of the thermal conductivity of the cometary surface layer can be derived from the TM data, evaluated together with data from the uppermost subsurface sensor of TP. In addition, during nighttime (without solar insolation) these measurements provide a quite accurate absolute estimate of the surface heat flux. However, to probe the conductivity locally over a wider depth and temperature range, the TP probe must supply the heat pulses directly to the ground.

[34] In order to measure the in situ temperature field in the medium, it is not necessary to rapidly scan the probe sensing temperature. Thermal cycling of the body goes in hours, the evolution in days, weeks and months. Heat diffusion is a slow process inside a bulk body on the scale of the probe. One should ensure however that the rate of sampling temperature on the scale of a single sensor must be faster and comply with the rate of thermal effects of the pumping.

[35] Initial tests of the probe performance were obtained by testing under vacuum with a background temperature of −160°C. These tests are also useful in quantitatively evaluating the thermal conductivity of the probe. Results of the vacuum heat pumping tests are shown in Figure 3, including the time-depth temperature map obtained with linear interpolation in distance dimensions. The temperature data are taken every ten seconds. The conclusion is twofold. The first is that only the heated sensor gets warm and the rate of heat propagation along the tube is low. The second is that, consequently, the disturbance by one sensor of the temperature measurement of another is small.

[36] The corresponding temperature increase is high, about 40–50°K, and reached within minutes, depending on the sensor since the sensors are not of equal area. The effects of the heat pumping in vacuum are felt by two neighboring sensors, and decay in about 30 min, i.e., about three times longer than the pulse width. The heater dissipates the heat only to the walls of the tube, and the outer walls then radiate into the vacuum. Only the sections adjacent to the heated unit are slightly warmed up due to the low thermal conductivity along the length of the probe.

[37] There are three different ways possible to operate the probe:



[38] 1. The first approach utilizes a single pulse on a specific sensor in order to probe the spatial distribution of thermal properties and their variation at the corresponding level. The medium is thermally sampled once or several times, on another level or in larger intervals. The purpose is to determine the spatial distribution of thermal properties and their variation in time, for example in different phases of a diurnal cycle. The choice of the time and the level of sampling have to ensure that thermal effects of one sample do not impact another. In this case a single pulse duration of several minutes is utilized.

[39] 2. The second approach utilizes several heat pulses in a series for continuous heating at a specific level, to average thermal effects in both the space and time. Heat is diffused and accumulated in this layer and is affected by the surrounding material, and above and below this layer. This results in effectively averaging any azimuthal inhomogeneity of the medium due to the azimuthal independence of the probe geometry. This approach may provide more accurate thermal properties measurements than the first technique described above but more for longer than shorter sensors. In this case a series of pulses will last a few tens of minutes.

[40] 3. The third approach utilizes a periodic pulse of heat sweeping along the axis of the probe for many cycles and over several sensors. The heat of the pulses is accumulated in a medium in all the levels along the probe resulting in an averaging of the effects in the medium. This effect approaches the method to the line source method (Healy, 76) because a series of many heated sensors is long. This approach is technically most difficult however. It may take hours to complete the sequence and in addition requires keeping heat dissipation uniform along the probe.

[41] These three approaches of operating the heat input to the medium are intended to confirm that particular effects present in the data repeat, or not, another time, and thus are relevant or irrelevant to a physical process. The measured data may be affected by unexpected conditions occurring in the test environment: (1) temporary electrical interferences; (2) preferential flow of the matter in local slots, caves, or holes; (3) retreat of the surface level due to loss of the matter; or other unknown conditions.

[42] Therefore it is useful to be able to operate the probe using different measurement procedures to confirm or exclude various measurement perturbations that might occur. When the probe is tested in the terrestrial environment the test conditions and environment may be directly examined for possible perturbations that may explain anomalous results. For cometary observations, little is known a priori about the conditions at the test site and having several different measurement approaches provides additional corroboration of a given set of measurements.

[43] The test results presented in this section were obtained in the laboratory using the space-qualified version of the instrument. The results presented in the next section were obtained with the copies of the probe not dedicated to be flown into space and with standard laboratory measurement equipment.

## 5. Timing Conditioning of the MUPUS-TP Probe

[44] Having measured only the bulk thermal conductivity is insufficient to determine the structure of the medium.

Information regarding the type of medium, its structure, texture and composition must be supported by other laboratory experiments and analytical approaches exercised even without direct relevance to cometary conditions. The goal of the present section is to show that observations using the probe require careful consideration of the timing between the heating and sensing cycles in order to correctly observe the evolution of thermal state and measure the thermal properties of the medium. This will be illustrated by the following examples.

[45] Timing related to the rate of bulk conduction and diurnal cycling on the comet is not required to be fast. Natural mass flows may be expected to be very fast on the comet due to the outflow of the matter, however. Simple tests conducted with the probe immersed in air and water show how the timing of the effects of measurements performed with the probe is related to the mass flow. Figure 4 shows the temperature effects, when the sensors are heated in open, quiet air and water. The selected sensor is heated in the interval (360 sec, left and middle; 120 sec, right) of pumping. During the interval a selected sensor is heated by a series of pumping pulses. The time of the series defines the sensing rate (once per 15 sec, left and middle; once per 5 sec, right). There are 24 series sent in one interval. Once per a series of pumping, all 16 sensors are sampled to determine the temperature.

[46] In the first example, when the probe is placed horizontally in quiet air, and set on heat pumping of a selected sensor, the pumped sensor is being warmed. The heat pulses cause the air to start flowing around the pumped sensor, with warm air outflowing and fresh air replacing the displaced warm air. As a consequence a neighbor of the heated sensor is cooled. The effect of temporary cooling is visible only on one side, due to some unresolved asymmetry in the configuration that affected the local air flow. It is visible over a time when the temperature values, from the compared sensors, are still correlated. In order to observe this effect in Figure 4 we have plotted the values read in each channel (1.16), as the increase of resistance values expressed in a normalized form. Each value in a channel is divided by the first value read in the same channel, when the pulse started. The relationship of the resistance increase to the temperature increase is given by the specific sensor sensitivity,  $2 \times 10^{-3}$ . If we were to plot using absolute temperature measure, the systematic errors related to particular sensors may hide the effects of cooling and warming.

[47] In the second example the same test is performed with the probe partially immersed into still water and results are shown in Figure 4 (middle). The sensors remaining in air above the water, behave the same as before. The responses from the sensors fully immersed in the water, are suppressed. Water, due to its higher thermal diffusivity compared to air, dissipates the heat effectively and thus the sensor is not getting warm when heated. Only the sensor staying partially in water behaves a bit differently.

[48] In the third example the sensors are fully immersed in water, but now set on faster heating and sensing, with a 5 sec rate that is three times faster than the previous test. This time we see that the pumped sensor is the coolest sensor of the probe (see Figure 4, right). This temperature decrease is temporary and small (1°C) but detectable. The water just warmed, started immediately flowing by convec-



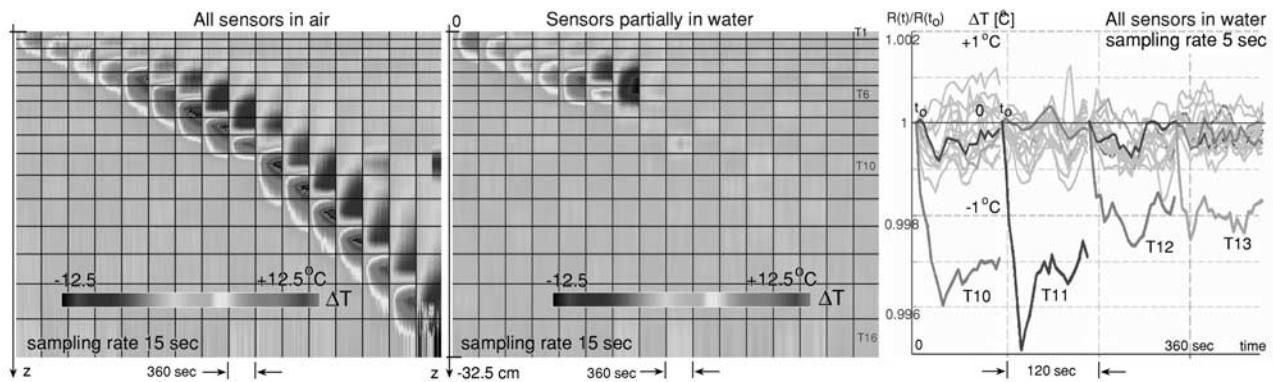


**Figure 4.** Effects of the heat pulsing when all the sensors are in open air (left), when the sensors are partially immersed in water (middle), and when the heated sensors are totally immersed in water (right). A sensor heated in water is evidently cooler than others when observed by the normalized change of resistance in time (right). The sensors not heated react mostly with uncorrelated noise and are shown in gray. The range of the temperature increase is  $\pm 12.5^{\circ}\text{C}$  for the maps (left and middle) and from  $+1$  to  $-2.5^{\circ}\text{C}$  (right). See color version of this figure in the HTML.

tion that brings in cooler water. When sensing the heated sensor was performed with the intervals three times longer, the short term effect of temporary cooling was missed. Then the effect is buried by the overall heat accumulation and uncorrelated noise. The same way as it happens in everyday experience with boiling water. This effect is visible as long as the correlation between temperature sensors exists. The correlation is determined by geometry, dimensions of the probe, medium properties and processes of the mass flow involved.

[49] The conclusion is that the time rate of the operation should match the rate of the mass flow to observe temporal effects of the matter flow. The aims of MUPUS-TP are limited to the first order effects of heat diffusion in bulk media. However, the mass flow will also be of concern in comet research. The apparent conductivity measured on the comet will include the effects related to thermal conductivity in the bulk matter, combined with effects of the matter flow. The contribution of the matter flow to the apparent bulk property is to be studied on the basis of a model of the flow, and verified by dedicated laboratory experiments.

## 6. Evidence of Latent Heat Effects

[50] The experiments with heating the sensors in air and water show the impact of mass transport on the thermal measurements. For the unique environmental conditions of a comet one must also consider the effects of latent heat. Due to the low-pressure environment of space surrounding the comet, only solid and gas phases are expected, no liquid phase. Heat input, from any source, may result in a phase change directly from a solid to a gas, with no direct change in temperature. This is due to latent heat. The input energy results in a phase change, not in an overall change of the thermodynamic temperature of the body. Other effects may come from the latent heat also visible by sensing the temperature state in a process excited from outside.

[51] The heat transfer brings a change of temperature. The change of temperature proves that transfer of sensible heat is involved. If the change of temperature stops or delays,

despite the fact that heat exchange is ongoing, then transfer of latent heat is involved. The amount of heat bounded or released depends on properties of the matter and the phase transition.

[52] It is possible to perform laboratory experiments on phase transitions under conditions of low pressure and temperature. However, since we do not have precise data on the cometary constituents, we have focused our studies on understanding the performance of the instrument, over what are believed to be conditions expected in the cometary environment.

[53] The simplest observation of latent heat is available under freezing and thawing the water ice, under quasi-isothermal conditions. The probe is inserted into a container of water and then the whole setup is frozen down to  $-50^{\circ}\text{C}$ , using a climate chamber. In our setup only eight of the sensors are scanned. The four bottom sensors (T13.16) are in water ice, the remaining sensors (T10.12 and T4) are left in air above the ice (see Figure 5). One of the top sensors (T4) is located is chosen far from the water ice in order to monitor ambient temperature in air. The sensors are sampled once per minute over a long period of about 40 hours while the test setup is left in the climate chamber (which is off) and exposed to ambient laboratory conditions, undergoing free quasi-isothermal warming. The chamber is off and serves only as a thermal enclosure.

[54] The results, shown in Figure 5, indicate an initial delayed phase of forming the warm ice lens (WI) initiated by the freeze before the tests. The warm ice lens is a form of that part of ice which expanded under freezing. The outside parts of deeply frozen ice thermally protect the inner parts and delay the heat from leaking out. After the freeze, the ice slowly starts warming due to the sensible heat transfer (SH). Next the ice is thawed as a result of the latent heat transfer (LH), and finally, the period of fast convection (FC) in liquid water terminates the process of melting the ice. The sample is warmed by the heat coming from all directions surrounding the container. The temperature change across the container is delayed differently at particular levels due to delay of the latent heat transfer. These temporal and spatial

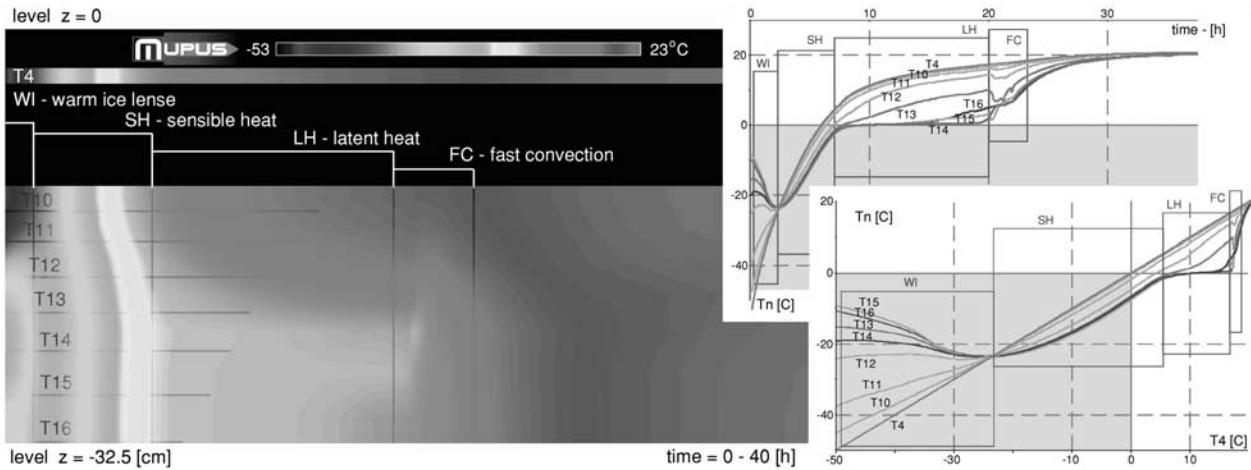


**Figure 5.** Experimental results of testing the MUPUS-TP probe under quasi-isothermal conditions using water ice thawing. The color map (left) shows the measurements due to eight sensors: T4, T10, T11, and T12 (measured in air) and T13–T16 (measured in water ice). The upper right rectangular plot shows the temperature-time history, and the lower right plot is the temperature state for each  $T_n$  versus ambient temperature as measured by T4. See color version of this figure in the HTML.

effects are clearly visible in the color temperature-space-time map in Figure 5. One can see how the boundary between the ice and liquid water proceeds in the 1-D spatial domain. The time history may be seen another way on the upper rectangular plot in Figure 5. The process proceeds exponentially in time. If we plot the temperature for each of the sensors,  $T_n$ , versus the specific reference temperature,  $T_4$ , corresponding to the ambient temperature, the results show the evolution of the temperature state with time as an implicit variable (see the lower right of Figure 5).

[55] This temperature state method is very useful not only for observing these types of processes but also for calibrating the sensors. The calibration may be performed in a similar manner, but with the probe surrounded by still air filling the climate chamber.

[56] The purpose is to sweep the thermal state of the probe in the range of temperature trying to keep all sensors in the same temperature or keeping the temperature gradient along the probe equalized. The sweep is possible under free isothermal warming. The warming proceeds at different rates in time, the slower the better. It depends on the heat capacity of the chamber, and the larger chamber the better. The heat transfer in the chamber passes at least once the zero gradient value in a long time and the related temperature is the concern for calibration. One needs at least three temperature states corresponding to  $T_{\max}$ ,  $T_{\min}$ , and  $T_0$  ( $=0^\circ\text{C}$ ) to determine a linear fit and anchor it in absolute values.

[57] The probe should be accompanied by two reference sensors to detect the zero gradient of temperature along the probe. Consistency of the sensors calibrated this way is better than  $0.05^\circ\text{C}$ . One may take as a rule of a thumb that in order to provide a good calibration, the temperature difference controlled by the reference sensors along the probe should not exceed  $\pm 0.3^\circ\text{C}$  over a distance of about 30 cm, resulting in a detectable gradient of about  $\pm 0.01^\circ\text{C}/\text{cm}$ .

[58] The intervals when the gradient is greater than  $\pm 0.3^\circ\text{C}$  over 30 cm are not taken into account for the

calibration. It is possible to find at least two temperature states with the gradient values sufficiently low to include the states into the calibration. Reproducibility of the sensitivity coefficients for all sensors integrated in one probe, even if they are different, is very good, while calibrating 16 separate sensors brings much worse consistency of the coefficients. Substituting the probe by many discrete sensors requires many conductors to connect them to the measurement system. A bound of conductors constitutes a considerable heat conducting path, which disturbs the zero gradient detection and makes the temperature states of particular sensors unequal. In effect the calibration becomes not trustworthy. Thermally the wires may disturb the calibration as well as the measurement tests.

[59] The effects with the ice test were too much dependent on the geometrical boundary conditions to analyze the heat exchange in absolute measure involving mass, energy and heat capacity of the specimen. The heat exchange occurred in all directions, not only parallel to the probe. A discussion of the effects of the probe geometry on the thermal property measurements is given in the next section.

## 7. Geometrical Configuration of the TP Probe

[60] The cylindrical probe has been designed for sensing the heat flowing in the direction normal to the surface. The probe comprises a hollow cylinder of the length  $l = 32.5$  cm, with the inner and outer radii  $a = 0.4$  cm and  $b = 0.5$  cm, respectively. The heat exchange between the probe and the surrounding environment can occur through any of its bounding surfaces, i.e., the inner and the outer walls or ring-like bases at  $z = 0$  and  $z = -l$ .

[61] In the model representing the expected temperature conditions on the comet, the material's temperature decreases exponentially from  $200^\circ\text{K}$  at the surface to  $100^\circ\text{K}$  at the depth where penetrator ends. The outer radius of the medium set in the model, is  $c = 1$  m, a distance large enough not to influence significantly the measurements of

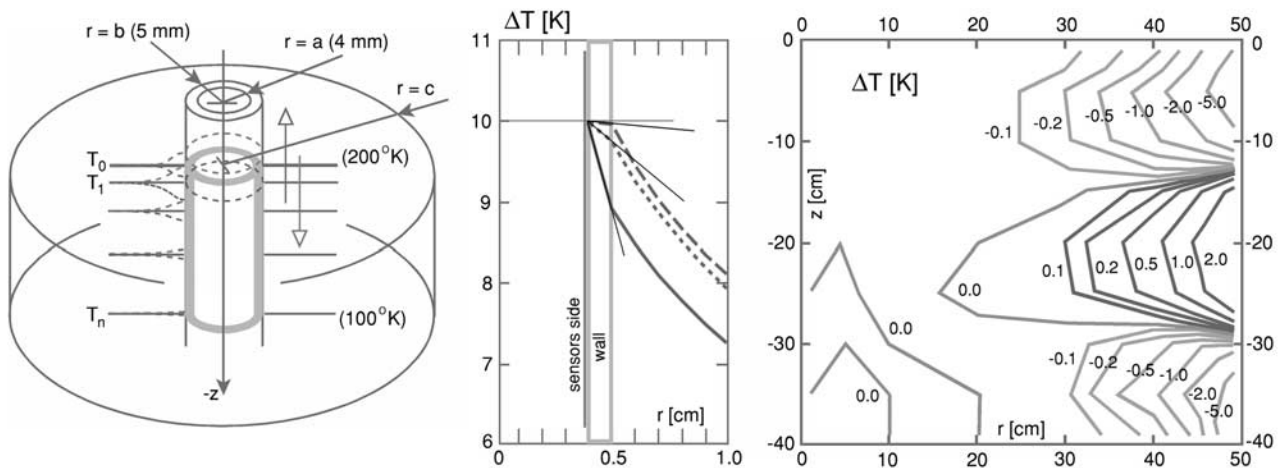


**Figure 6.** A geometrical configuration of the probe in the medium with the expected isotherms sketched (left). The temperature across the wall is shown in a near vicinity of the tube (middle). The map showing estimated errors of the temperature measurements versus radial distance from the probe (right). See color version of this figure in the HTML.

the sensors. Intuitively one can expect that the isotherms inside the medium  $T_0, T_1, \dots, T_n$  (see Figure 6, left), might be perturbed by the presence of the hollow and the probe, especially in the case of heat transfer along the tube. However, the moderate thermal conductivity of the tube (0.5 W/m/K) and its small overall thermal capacity (small mass and volume) normally makes perturbations important only in the short initial time interval ( $<1$  min) necessary to accommodate the thermal state of the probe to that of the medium. Only a very unusual, forced heat transfer along the tube (e.g., by external heating from the top) can significantly influence the medium near the tube and corrupt sensor measurements.

[62] The heat exchange is provided by the surface and bottom planes,  $z = 0$  and  $z = -l$ . The temperature state is  $200^\circ\text{K}$  for the top, and  $100^\circ\text{K}$  for the bottom according to the conditions expected on the comet. It is imposed that the probe senses temperature radially. It feels the state of the medium inside a corresponding cylindrical volume of the radius  $r = c$ . Intuitively one can expect that the isotherms inside the medium  $T_0, T_1, \dots, T_n$  (see Figure 6, left) might be perturbed by the presence of the hollow and the probe. Determination of the isotherms is not a good point for the analysis however.

[63] There are two possible approaches to the analysis of temperature profiles measured by sensors. In a so-called direct problem, one wants to know the temperature values of the sensors implied by the initial conditions (temperature distribution in the medium) and thermal boundary conditions on the top ( $z = 0$ ), and the bottom ( $z = -l$ ) as well as on the cylindrical sides corresponding to (1) the sensors at  $r = a$ , (2) the probe at  $r = b$ , and (3) the outside at  $r = c$ . The second approach is an inverse problem, in which one wishes to determine temperature values at the outer boundary of the medium ( $r = c$ ), taking the sensor temperature values from a measurement.

[64] The direct and inverse problems were solved by Hagermann [1999] and Hagermann and Spohn [1999]. Recently it was solved also by M. Banaszkiewicz (unpub-

lished data), who employed the Green function method. In particular, he was able to determine the material's temperature at the maximum radius  $r$  that varied in dependence of assumed thermal properties of the medium. In both problems the boundary conditions for  $r = a$ , corresponding to the sensors have been (arbitrarily) taken as adiabatic. At the penetrator-medium boundary,  $r = b$ , the continuity of temperature and heat flux is assumed. One of the specific results of the analysis gives the temperature drop across the tube wall. The analysis of the temperature distribution was made for the assumed thermal conductivity of the medium of  $0.04$  W/m/K, i.e., the likely value of the porous, cometary material. When the temperature state is under a stationary process while sensing then the temperature drop across the wall is only  $0.05^\circ\text{K}$  (Figure 6, middle). However, the value is much dependent on the property of medium.

[65] Another result of the analysis was to estimate the distance where the probe can still sense the medium. The uncertainty of sensing as a function of distance is shown in Figure 6 (right), being a result of the following numerical experiment. Initially, the sensor's temperature varies linearly from  $200^\circ\text{K}$  at the top to  $100^\circ\text{K}$  at the bottom. The sensor temperature varies in time, until it matches the given exponential temperature profile in the medium. Assuming random measurement errors with an amplitude deduced from the sensor specification (resolution  $0.025^\circ\text{K}$ ), it was possible to determine the profile in the material by employing the least squares method.

[66] Practically, the volume of the medium that can be sensed is large. The probe 32.5 cm long has a wall area of  $1$  dm<sup>2</sup>, and senses a volume of about  $25$  dm<sup>3</sup>, according to estimations performed for typical thermal parameters of a cometary nucleus. Another explanation for the limited impact of the wall on sensing is the total heat capacity of the tube with sensors, is small with respect to the total heat capacity of a large cylindrical volume filled by the medium under sensing.

[67] A crude experimental check was performed in terrestrial soil. While sensing temperature with 12 sensors,



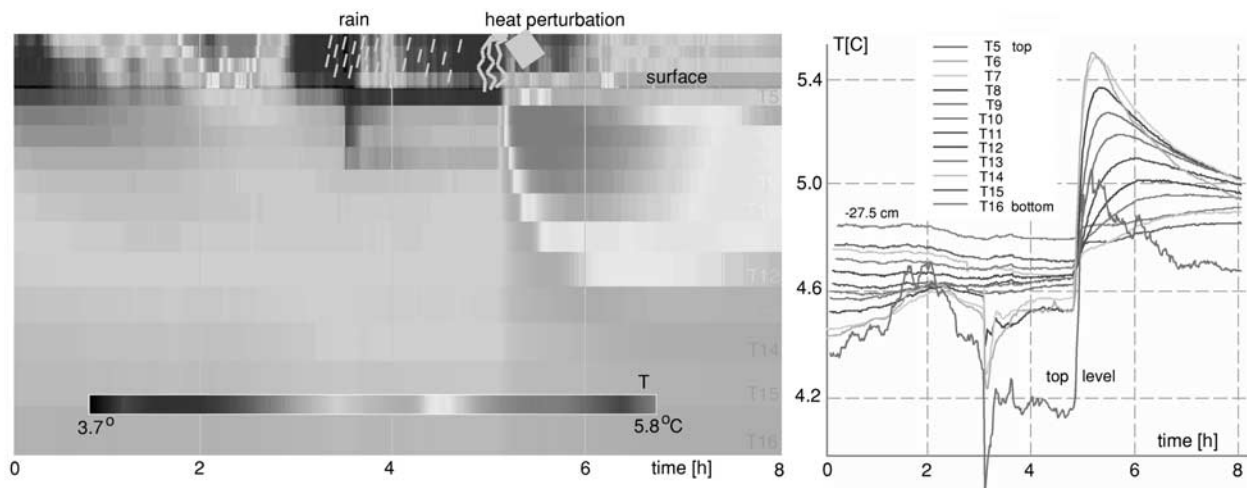


**Figure 7.** Plot of temperature data measured every minute by 12 sensors in soil, showing that the heat perturbation introduced to the soil (with 0.25 l of water, 15°C) at a distance of 0.50 m from the probe (in the time = 5 h) is evidently sensed: the temperature map (left) and the xy plot (right). See color version of this figure in the HTML.

heat perturbation was introduced pouring a cup of water (0.25 l, at 15°C) onto the ground at a distance of 50 cm from the probe. The effects of the heat injection (see Figure 7) with water infiltration are evident on all the sensors for hours, though the perturbation was relatively small with respect to the heat capacity of soil inside the cylinder of radius 50 cm. The deduction of a sensing distance from this experiment appears a bit questionable due to capillary forces taking the water around everywhere in the soil but the comparison of the heat capacity of the soil in the cylinder volume to the heat capacity of the introduced water proves roughly that the probe really senses temperature widely around.

[68] The same analysis of direct and inverse problems can be used to estimate the effects of sensor heating. The question of how precisely one can determine thermal conductivity of the medium must involve the 2D time-dependent heat conduction equation in the geometry, introduced earlier (Figure 6, left), as well as analysis of measurements themselves (i.e., errors in determining the temperature from electrical measurements of voltages and currents in the sensor circuit).

[69] Taking equation (1), one would expect very high precision adequate for a 16-bit resolution control system. However, the electrical variables themselves do not exclusively determine the thermal conductivity measurements. Equation (1) describes only the pure case of a linear heat source. The proper equivalent of the equation for the real TP probe does not exist yet. Currently we cannot provide an exact estimate of the precision. Typical accuracies with line heat source probes are around 5–20%.

## 8. Experiments in a Terrestrial Snow Environment

[70] The simple experiments with water ice previously discussed provided evidence for the applicability of this technique for determining the thermal properties of terrestrial snow and ice.

[71] The program EXTASE (“An EXperimental Thermal probe for Applications in Snow research and Earth sciences”) has been ongoing since 2001 with this goal. The first measurements in snow were performed from 20 May through 3 June 2002 at Spitzbergen (Svalbard, Ny-Ålesund, Kongsfjorden) by K. Schröder in cooperation with the Alfred-Wegener-Institut (AWI) in Bremerhaven. The goals and results of the experiments are described in the reports by Haas *et al.* [2002] and Schröder *et al.* [2002].

[72] While the physical state and origin of terrestrial snow and ice are different from that expected for a comet, the same principles of heat exchange and phase transitions apply in both domains. The experimental setup for the tests in snow was arranged to allow for long-term observations of the temperature state that would include daily cycling. The season and the time of the observations were chosen about two weeks before the period of most intensive thawing. The beginning of the spring is the beginning of the polar day in Spitzbergen. The tests started when the ambient temperature was low, around  $-20^{\circ}\text{C}$ . Figure 8 demonstrates that the effects of the daily cycling are observable down to about 20 cm below the snow surface. On 21 May 2002, when the probe was set vertically in the snow, the snow cover overlying the sea ice substrate was about 25 cm thick. By 3 June 2002 the snow cover had been thinned, and was only about 10 cm thick. The profiles inside the snow are increasingly bound together in a range of daily temperature changes with increasing depth. The probe was inserted vertically into the snow except on 3 June (Figure 8, far right plot), when it was inserted diagonally with a tilt angle of 33 degrees to the surface.

[73] Just as the terrestrial snow material is lost from the surface, we expect similar mass loss in the cometary environment. We expect to be able to observe this mass loss on the comet using the probe observations. For the terrestrial snow, the mass loss was observed using the probe temperature variations over the many days of data collection. It was not possible to determine precisely the actual surface position from the probe data. The data



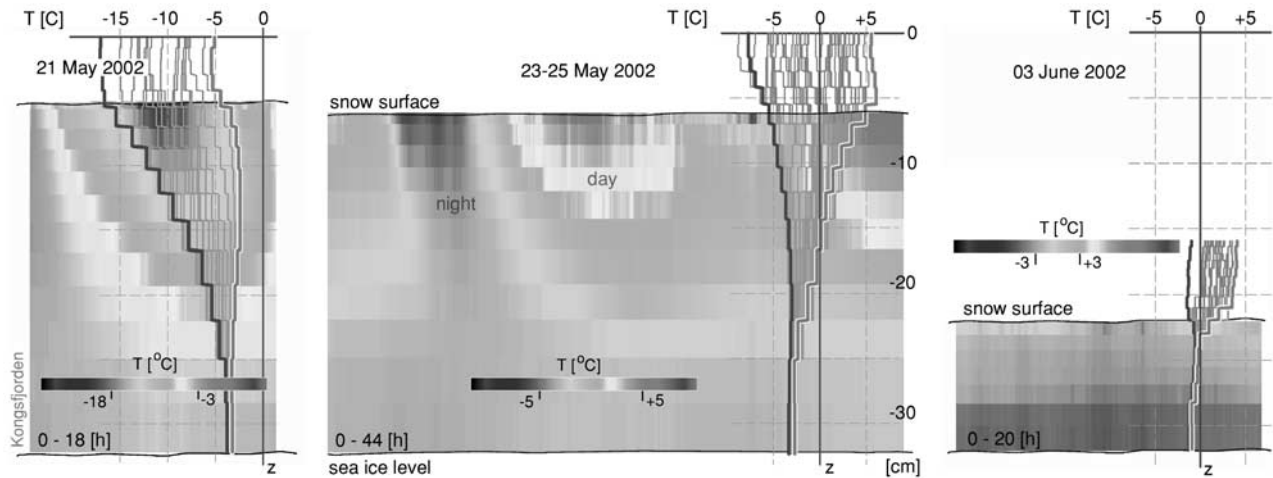


**Figure 8.** Temperature profiles plotted once per hour during the three days showing the evolution from the cold to the warm weather. The line plot of temperature,  $T$ , in a panel refers to the vertical axis  $z$  initially located as  $z = 0$  at the top sensor in the probe. The cross section of the snow layer is filled with the map showing temperature versus time with a time elapse from left to right. The palette indicates the range of employed colors. The probe was scanned every 5 min. See color version of this figure in the HTML.

from the probe sensors above the snow are contaminated by convection, advections and by heating due to incoming solar energy. The surface location cannot be determined to an accuracy better than the spatial resolution, i.e., the length of a single sensor. However, above the surface of a comet essentially there is no atmosphere, dense enough to observe similar contamination by convection. Therefore the surface loss of material could be detected there.

[74] Since snow is semi-transparent to the incoming radiation, the sensors below the surface feel the effects of

this radiation. We also observed that the snow around the probe had melted in the vicinity of the air-snow interface, leaving the upper portion of the probe standing in a conical hole depleted of snow. It was also observed that the lower sensors which were deeper into the snow layer suffered from poor thermal contact with the snow, as evidenced by the difference in temperature readings between neighboring sensors. Then, corresponding values diverged much one sensor from another. For the terrestrial snow observations the probe was painted white, and for the cometary measurements the probe is painted black.

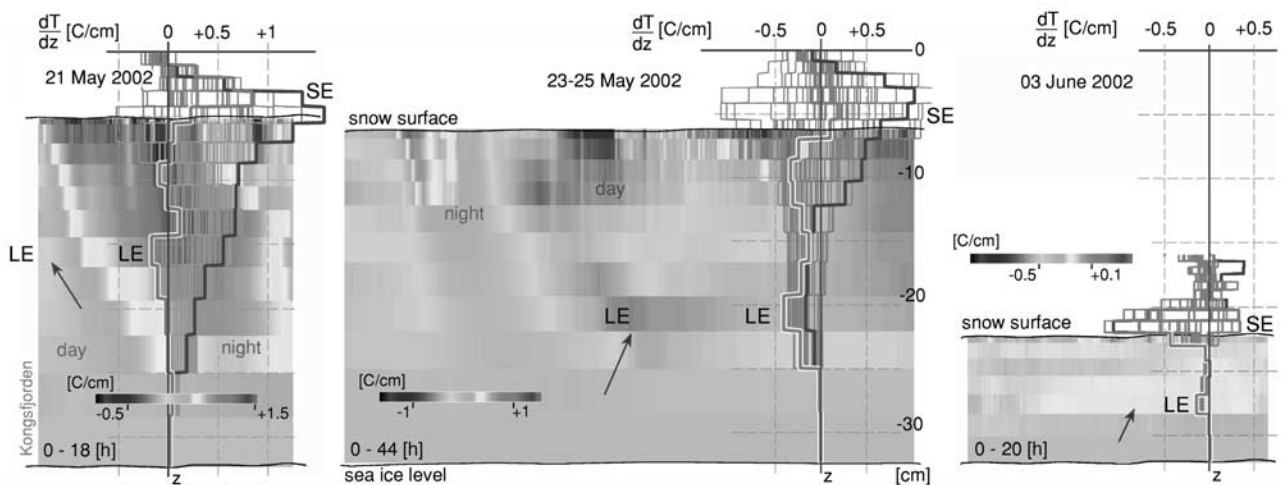


**Figure 9.** Temperature gradient profiles in snow corresponding to the data plotted in Figure 8. The maximum in the absolute value of the gradient corresponds to the surface location. Negative gradient values imply downward heat flow, and positive values imply upward heat flow. Local extremes of the gradient are denoted by SE (Surface Extreme) and LE (internal Layer Extreme). The extremes of type LE mean that a sensor is warming more from the top than the neighboring sensors. See color version of this figure in the HTML.

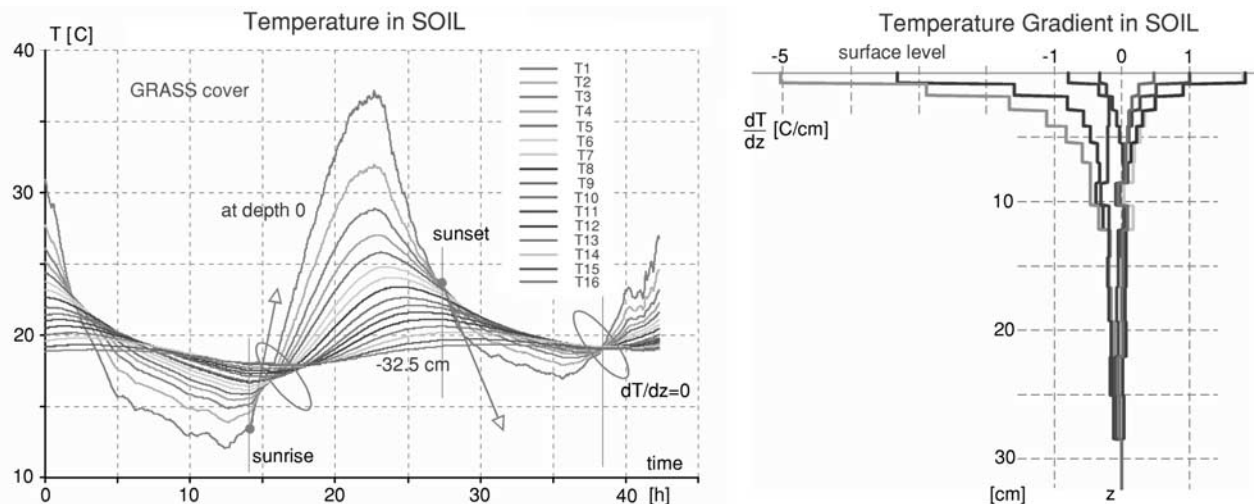


**Figure 10.** Typical temperature cycles (left) and temperature gradients (right) measured in soil under strong solar irradiation conditions. The temperature data values were taken every minute. Profiles of the gradient are plotted every six hours. See color version of this figure in the HTML.

[75] The temperature gradient in snow is low due to its large heat capacity. It is confirmed by the probe observations shown in Figure 9. The gradient data,  $dT/dz$ , obtained during a period of intensive melting, is very flat. Only the temperature gradient values close to the surface are large. A positive temperature gradient means that the heat flows up during the nightly cooling and a negative temperature gradient means that the heat flows down away from the surface with the daily warming.

[76] Observing the temperature gradient values deeper than 10 cm below the surface, one can identify a local negative extreme in the gradient. This extreme is evident, and repeats day by day, during both the cold and the warm days. The extreme is a result of the heat input from the surface. It is believed that the heat comes with liquid water from the melt layer at the top of the snow. Water melts at a surface, flows down into the snow where it freezes at the lower temperature. This phase change results in the release latent heat that is observed by the sensor as local increase in the negative temperature gradient. The sensors lying above this location do not experience any heat exchange since the liquid water just flows past until it reaches the location where it freezes.

[77] A similar effect was observed when the ambient temperature was as low as  $-20^{\circ}\text{C}$ , consistent with the daily warming cycle. It may be possible that those particular grains of snow are melted under the temporary increase of pressure, which appears locally on facet interfaces between the grains, due to the thermal extension of the snow during a day and under the weight of the snow in a long trend. The effect is very small but detectable with the probe. The relevance of this effect to the metamorphosis of snow must be demonstrated quantitatively by additional experiments.

[78] A general conclusion is that the data keep the integrity well in relevance to the processes in spite of the complications due to the changing surface level and temporarily poor contact of the probe with the snow at the surface level. Contamination of the data by effects of radiation, convection and advection in the air, which are

common complications in snow research, do not destroy the relevance to physics. The data were also much contaminated by other unresolved effects likely introduced in the electromagnetic waves from the ionosphere above the test site in the polar region but they are not visible on the temperature maps shown above though they are present in the data. The large area of the probe and its capability for azimuthal averaging constrain the impact of the contaminating effects to some degree.

## 9. Experiments in a Terrestrial Soil Environment

[79] The TP probe was extensively tested in terrestrial soils. Two of the tests are discussed in the following. Results of the first one are presented in Figure 10 to show the temperature effect in soil during clear weather with strong insolation. Results of the second are depicted in Figure 11 and show the effects on the heat fluxes in soil during very poor insolation conditions. Only the second experiment was chosen for presenting the heat fluxes because it is well known that most of the flux measurement methods commonly used fail or are not trustworthy under low exchange of energy conditions.

[80] The MUPUS-TP experiment is primarily intended to study thermal properties by temperature and thermal conductivity of a medium. The same experiment may also provide a good understanding of energy budget within the medium, an area also of interest in the soil research communities. In soil research the energy budget is recently even the first concern when considering of the global climate change on Earth. A use of the TP probe for this purpose is possible and was aimed for the following experiments in soil.

[81] The trouble was that the version of the TP probe utilized for the terrestrial experiments was not yet equipped with all the power control electronics, which is necessary for long-term operation in the open field. Therefore the direct determination of the conductivity by active heating was not possible in these tests. The probe employed only

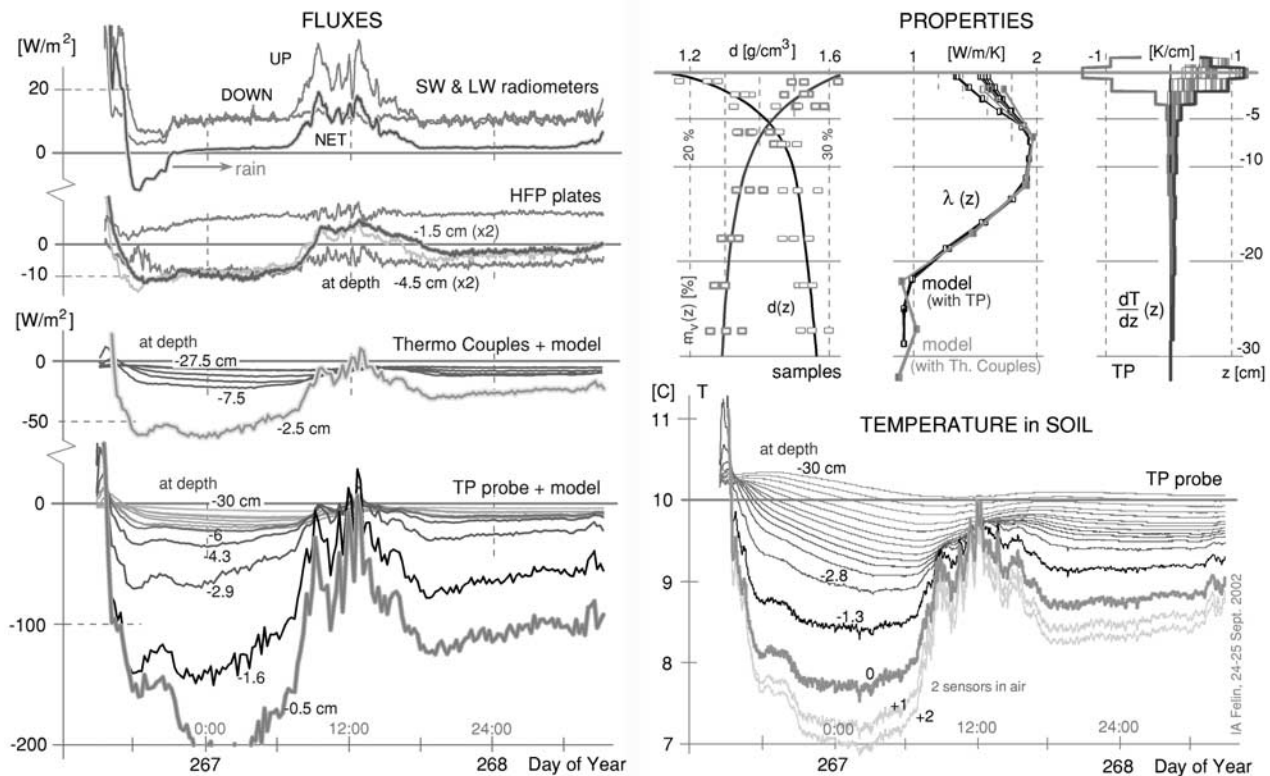


**Figure 11.** Comparison of heat fluxes (left panel, fluxes) measured by different methods and relevant data with the profiles of soil properties: the volumetric soil moisture  $m_v(z)$ , the thermal conductivity  $\lambda(z)$ , the temperature gradient  $dT/dz$  (top right panel, properties), and the temperature values measured at the test site by the TP probe (bottom right panel, temperature). See color version of this figure in the HTML.

the mode of sensing. In order to determine energy fluxes within the soil the thermal conductivity is desired however. The conductivity was thus derived from other physical measurements. So the following soil tests were undertaken with the goals inverted.

[82] In the past the underground heat flux was measured in a similar way for geothermal research, namely by determining the temperature gradient as shown by *Christoffel and Calhaem* [1969]. The new aspect in the presented method, is that we determine the gradient by a complete and consistent profile of temperature over the range of depth,  $T(z)$ , by sixteen sensors, not only by two measurement points.

[83] An alternative method is the so-called “zero temperature gradient time and depth” below the soil surface. The method is described by *Kimball and Jackson* [1975]. This technique measures the time dependence of the temperature and the temperature gradient a few cm below the surface over a diurnal cycle. The zero temperature gradient means that the heat flow across this subsurface level apparently stops for a while or is balanced to zero. Both methods require a knowledge of the thermal conductivity.

[84] According to *Kimball and Jackson* [1975], the zero gradient method refers to the zero flux value. Both methods employ an external heat stimulus. The present method also employs an external heat stimulus but only to determine the temperature gradient and rely on heat exchange from the own power sources to determine the conductivity.

[85] The TP probe indicates the zero gradient very clearly as shown in Figure 10 (left). The temperature state of all the close subsurface layers is nearly equalized at the time of sunrise. This typically occurs at about sunrise at the locations in Poland where the test was performed, and at the similar latitudes. It may be noted that peak values of the temperature in the day time indicate well thermal inertia in different layers.

[86] Another method commonly employed for heat flux measurements is known as the method of heat flux plates (HFP). The HFP method utilizes a flat stack of many thermocouples that capture the transient heat flux diffusing across the plates, as if through an aperture. There are many difficulties associated with the HFP method. The plates require good thermal contact to the medium under study and moreover the HFP method requires matching the thermal conductivity of the plates to the soil thermal conductivity. If these conditions are not met then the plates depress the isotherms of the temperature field significantly and provide a large measurement errors. Another known disadvantage is that the plate stops the mass flow in the area of cross section. The HFP plates work poorly with small fluxes, less than  $30 \text{ W/m}^2$ .

[87] The MUPUS-TP probe is another alternative to HFP measurements in that it applies the gradient method. Like other gradient methods, our probe with its small cross section area does not block the heat and mass flow around it. Due to its relatively low thermal conductance, MUPUS-



TP also reduces the risk of thermal short-circuiting and has the additional advantage of measuring the thermal profile at high spatial resolution.

[88] The energy flux is a multiplication product of the thermal conductivity of a medium and the related temperature gradient. The conductivity was possible from other soil research utilizing a thermal model of soil. We used the model developed by *Usowicz* [2002]. This model provides the conductivity value while it is fed with input data determining several properties of the soil and temporary conditions. Among the required conditions there is the temperature state measured on the test site and its time evolution. The temporary temperature values were supplied to the model from two independent sources: (1) the values measured by a series of thermocouples and (2) the values measured by the MUPUS-TP probe.

[89] Results of the model are shown as the profiles of the conductivity  $\lambda(z)$  [W/m/K] in Figure 11 (panel “properties,” middle). The conductivity values obtained from the model are computed using the temperature measured alternately by the thermocouples and by the probe. The conductivity depends on the temperature but only weakly. The differences of the conductivity values determined by the two different methods (TP probe and thermocouples) are very small despite considerable differences of temperature between the measurement means. The profiles of  $\lambda(z)$  are stable and vary slightly in the near subsurface layers over the time of the experiment.

[90] The model is based on the assumption that the soil is a mixture of spherical grains contacting one to another. Several compounds were determined by the independent analysis of grains. Each compound has its own volumetric statistics for the grain size. The number of contacts between small and large grains determines the value of thermal conductivity and depends on the grain size distribution function. The model depends on temperature, soil moisture, salinity, dielectric constant and water potential in the soil, and all these parameters were employed. It is also possible to take into account the effects of the water evaporation and condensation but the related measurements of the water vapor partial pressure were not performed during the test. The model was finally calibrated and thoroughly checked using a broad range of representative soil types and their thermal behavior under different environmental conditions. Results of the calibration procedure are described by *Usowicz* [1995].

[91] The test for determining fluxes in soil with the TP probe was accompanied by three other independent flux measurement means: (1) the setup of the HFP plates to measure the fluxes directly in soil; (2) the set of thermocouples plus the thermal model, where by the same thermal model was employed for the TP probe; and (3) the short-wave (SW) and long-wave (LW) radiometers to monitor the incoming and upwelling radiation. The fluxes measured and evaluated in the test are shown in Figure 11 (panel “fluxes”).

[92] The fluxes measured by the LW and SW radiometers prove well that the weather during the tests was steadily poor, probably due to the autumn season at the location. During the period of the measurements the day and night sky was fully covered by heavy clouds and it there was considerable rainfall. This resulted in low values for the net radiation of  $20 \text{ W/m}^2$  (NET), in a peak value.

[93] The fluxes measured by the HFP method indicated values in the range of about  $\pm 10 \text{ W/m}^2$ . Four HFP plates were used, in pairs at different depths of  $-0.5 \text{ cm}$  and  $-4.5 \text{ cm}$ , to confirm repeatability. Figure 11 (panel “fluxes,” second from top) contains only the HFP fluxes from one of the test sites while the tests were performed at two different sites with very similar results. Among all only one of the plates indicated an offset uncertainty of about  $10 \text{ Watts/m}^2$ . The obtained fluxes were considered as non-trustworthy because the values fall below the range of the typical sensitivity of the HFP plates.

[94] The fluxes determined on the basis of the thermocouple data and the model, seemed to give a better fit to the expected values, reaching a peak of about  $-60 \text{ W/m}^2$  (see Figure 11, panel “fluxes,” third from top) during the first night of the test. The weather suggests that strong cooling should be expected.

[95] The instantaneous heat fluxes outgoing from the soil measured with the TP probe and the model even reached  $-200 \text{ W/m}^2$  at the surface. With these means the effect of cooling was unexpectedly large. The value does not correspond to the measured net radiation and the HFP method results. The moderately sunny day preceding the tests may provide some partial explanation. One may understand that during the first night the soil released the heat accumulated during the previous day but the upwelling heat continuously lasting during the second night is still much greater than the heat flux measured by thermocouples. The time of the flux test is too short to expect a seasonal trend. The high rate of the upwelling heat flux assessed with the TP probe may be understood as likely over estimated but not by the factor of three, as suggested by comparing the flux from the probe at  $-0.5 \text{ cm}$  to the flux from the thermocouples at  $-2.5 \text{ cm}$ .

[96] Differences of the temperature values obtained from the probe and the thermocouples do not impact the conductivity values as it was shown by the profiles  $\lambda(z)$  [W/m/K] (see Figure 11, panel “properties”). However, the differences of the temperature gradient values between the means were considerable. The TP probe provided a gradient up to  $1.2^\circ\text{K/cm}$  of the peak value at the surface level while the thermocouples indicated only about  $0.6^\circ\text{K/cm}$ , the peak value at a depth of  $-2.5 \text{ cm}$  that is in the range of the steepest gradient values. The TP probe gave a gradient gradually changing with depth, while the gradient from the thermocouples varied only weakly (and inconsequently) with depth. The temperature gradient determines the flux directly when multiplied by the conductivity, not affecting the values of conductivity. It provides some explanation that the fluxes, derived from the probe are greater than those derived from the thermocouples.

[97] The thermocouples are not sufficiently trustworthy, however. The gradient measured by them was surely less precise, because the related temperature resolution is not better than  $0.1^\circ\text{K}$ . The gradient obtained with the TP probe was very much more consistent among all layers and more precise, due to the better temperature resolution of the probe ( $0.05^\circ\text{K}$ ). A possible cause of the overestimation with the probe may be attributed to the precision of the temperature gradient determination. The most intensive flux is measured close to the surface, where the gradient depends strongly on a proper identification of the surface level. The estimate of the surface level was in fact limited to about  $5 \text{ mm}$  due to



roughness of the soil surface and the thermally apparent thickness of the grass vegetation cover. A thermal estimate of the surface level from the temperature data relates also to the disturbance of the temperature field by the hollow filled with the probe, where no corrective functions were used due to the thick geometry of the top sensors in the probe.

[98] More unresolved issues may be related to water vapor exchange, which was not monitored during the test. The flux values obtained with the TP probe are believed to be reliable likely. It is worth noting that this large contribution due to atmospheric heat exchange is provided by the convection and advection in the air. This component of the energy balance is not detectable by the radiometers since it does not involve the emission of infrared radiation.

[99] Finally there are two conclusions from the tests in soil. The first one is that the precision of the energy flux determination strongly depends on the precision of the temperature gradient measurement. However, even if one has a perfect tool for determining the temperature gradient, the derived heat flux may be still highly impacted by the unresolved contribution of other effects involved the heat transport with mass flow and latent heat transfer, if not sufficiently represented by the thermal conductivity. The second conclusion is that the TP probe more sensitively measures weak energy fluxes compared to the common method of the HFP plates.

[100] The results of the tests in soil show enormously large discrepancy between the methods of determining the heat fluxes under natural conditions. This is a common and very regular experience considering fluxes. We believe that the precision of determining the thermal conductivity is at least as difficult as the precise determination of the heat fluxes.

[101] A determination of the atmospheric component of the total energy budget in terrestrial conditions is of interest to agrophysics. In general this type of measurement has to rely finally on analysis using models developed for computing the circulation of water and gases in a terrestrial environment. Despite the differences due to the unique characteristics of various planetary bodies, there are many commonalities in the tool used for these studies.

## 10. Conclusions

[102] In this paper we have demonstrated the following:

[103] 1. The MUPUS probe is an efficient research tool for measuring subsurface thermal properties and temperature profiles.

[104] 2. Adequate temporal and spatial resolution of the thermal measurements is required for understanding the physical processes of the sampled media.

[105] 3. The probe should be used in a way complying with the direction of the heat flux flowing parallel to the probe.

[106] 4. The sampling rate of the measurements should be greater than the timescale for the dynamics of the heat exchange.

[107] 5. The probe is suitable for the investigation of the thermal properties of inhomogeneous media.

[108] 6. The probe is also suitable for sensitive measurement of the heat fluxes under poor insolation conditions.

[109] We have also demonstrated that the use of the probe, in conjunction with appropriate thermal models, allows for a

great understanding of the thermal properties of the media under investigation.

[110] **Acknowledgments.** We would like to thank our colleagues from the MUPUS team not involved directly in preparing this paper for seven years long, fruitful cooperation on developing the instrument, many stimulating discussions, and continuous interest in technical as well as scientific matters related to the method. In particular, we are in debt to Norbert Kömle from the Institut für Weltraumforschung in Graz, who helped us a lot in clarifying issues concerning heat and mass transport in comet-like materials. Among the persons deserving special thanks are Jacek Leliwa-Kopystyński and Konrad Kossacki from the Institute of Geophysics, University of Warsaw and Ryszard Walczak from the Institute of Agrophysics, Lublin for their deep interest about the subject and reliable support with performing the environmental tests of the method. Another exceptional contribution that should be notified was brought by Tadeusz Kowalski from SRC, Warsaw. His skills and knowledge in chemical processing of Kapton made the design of the sensors feasible. We would like to express our gratitude to two referees of the paper who have thoroughly read it and suggested many changes that improved its quality. We owe special thanks to Samuel D. Gasster, the Aerospace Corporation, Los Angeles, who generously devoted his time to correct the language of the original manuscript, made the paper readable, and assisted to complete it with great patience and understanding of the subject. The work was supported from the Polish State Committee for Scientific Research grant 5 T12E 027 25. We also acknowledge partial support by the Austrian "Fonds zur Förderung der Wissenschaftlichen Forschung" under project P15470.

## References

- Banaszkiewicz, M., K. Seiferlin, T. Spohn, G. Kargl, and N. I. Kömle (1997), A new method for the determination of thermal conductivity and thermal diffusivity from linear heat source, *Rev. Sci. Instrum.*, **68**(11), 4184–4190.
- Christoffel, D. A., and I. M. Calhaem (1969), A geothermal heat flow probe for in situ measurement of both temperature gradient and thermal conductivity, *J. Phys. E, Ser. 2*, **2**, 457–465.
- Gregorczyk, W., B. Jancewicz, and W. Marczewski (1999), Titanium thin film thermometric sensors on multilayered Kapton foil substrate for the experiment MUPUS of the ESA cometary mission Rosetta, paper presented at 23rd International Microelectronics and Packaging Society (IMAPS) Conference, Kolobrzeg, Poland.
- Haas, C., J. Bareiss, and M. Nicolaus (2002), The surface energy balance and its importance for superimposed ice formation (SEBISUP), report, *LSF Proj. NP-9/2001*, Alfred-Wegener-Inst. für Polar- und Meeresforschung (AWI), Bremerhaven, Germany, June.
- Hagermann, A. (1999), Die Ermittlung des oberflächennahen Temperaturfeldes aus einer gestörten Gradientenmessung: Zur Inversion planetarer Wärme-flussmessungen unter besonderer Berücksichtigung des Experiments MUPUS PEN-TP, Ph.D. thesis, Westfälische Wilhelms-Univ. Münster, Münster.
- Hagermann, A., and T. Spohn (1999), A method to invert MUPUS temperature recordings for the subsurface temperature field of P/Wirtanen, *Adv. Space Res.*, **23**(7), 1333–1336.
- Healy, J. J., J. J. de Groot, and J. Kerstin (1976), The theory of the transient hot-wire method for measuring thermal conductivity, *Physica C*, **82**, 392–468.
- Keihm, S. J. (1984), Interpretation of the lunar microwave brightness temperature spectrum: Feasibility of orbital heat flow mapping, *Icarus*, **60**, 568–589.
- Kimball, B. A., and R. D. Jackson (1975), Soil heat flux determination: A null-alignment method, *Agric. Meteorol.*, **15**, 1–9.
- Kömle, N. I., G. Kargl, K. Seiferlin, and W. Marczewski (2002), Measuring thermo-mechanical properties of cometary surfaces: In situ methods, *Earth Moon Planets*, **90**, 269–282.
- Rohlf, K. (1986), *Tools of Radio Astronomy*, pp. 7–14, Springer-Verlag, Berlin.
- Schröer, K., K. Seiferlin, T. Spohn, W. Marczewski, and S. Gadowski (2002), EXTASE: An experimental thermal probe for applications in snow research and earth sciences—Project concept and first results, IfP report, Inst. für Planetol., Münster, Germany.
- Seiferlin, K., N. I. Kömle, G. Kargl, and T. Spohn (1996), Linear heat source measurements of the thermal conductivity of porous H<sub>2</sub>O-ice, CO<sub>2</sub>-ice and mineral powders under space conditions, *Planet. Space Sci.*, **44**, 691–704.
- Spohn, T., J. C. Zarnecki, N. I. Kömle, K. Ekkehardt, J. Benkhoff, K. Seiferlin, M. Banaszkiewicz, and G. Kargl (1995), Proposal for a suite of instruments to make in-situ physical measurements at the surface of a comet nucleus, pp. 1–37, MUPUS, Inst. für Planetol., Münster, Germany.

- Usowicz, B. (1995), Evaluation of methods for soil thermal conductivity calculations, *Int. Agrophys.*, 9(2), 109–113.
- Usowicz, B. (2002), The universal model of mass and energy transfer in a porous medium, 17th WCSS, Bangkok, symposium no 4, paper 275.
- 
- A. J. Ball and A. Hagermann, Planetary and Space Sciences Research Institute (PSSRI), Open University, Walton Hall, Milton Keynes MK7 6AA, UK. (a.j.ball@open.ac.uk; a.hagermann@open.ac.uk)
- M. Banaszkiewicz, S. Gadowski, J. Grygorczuk, M. Hlond, J. Krasowski, and W. Marczewski, Space Research Centre, Polish Academy of Sciences, ul. Bartycka 18A, 00-716 Warsaw, Poland. (wmar@cbk.waw.pl; sgadomsk@cbk.waw.pl; jurekgry@cbk.waw.pl; mhlond@cbk.waw.pl; jack@cbk.waw.pl)
- W. Gregorczyk, Telecommunication Research Institute, PIT, ul. Poligonowa 30, Warsaw, Poland. (greg@pit.edu.pl)
- G. Kargl, Institut für Weltraumforschung der ÖAW, Schmiedlstraße 6, 8042 Graz, Austria. (guenter.kargl@oeaw.ac.at)
- J. Knollenberg and E. Kührt, DLR Institute of Planetary Research, Rutherfordstrasse 2, 12489 Berlin, Germany. (joerg.knollenberg@dlr.de; ekkhard.kuehrt@dlr.de)
- K. Schröder and T. Spohn, Institut für Planetologie, Westfälische Wilhelms-Universität Münster, Wilhelm-Klemm-Str. 10, Münster, 48 149, Germany. (kathrin.schroeder@uni-muenster.de; spohn@uni-muenster.de)
- K. Seiferlin, Physikalisches Institut, Sidlerstrasse 5, 3012 Bern, Switzerland. (karsten.seiferlin@phim.unibe.ch)
- B. Usowicz, Institute of Agrophysics, P.O. Box 201, ul. Doświadczalna 4, 20–290 Lublin 27, Poland. (usowicz@demeter.ipan.lublin.pl)